J Therm Anal Calorim (2012) 107:489–498
DOI 10.1007/s10973-011-1531-8

Study on optimization of hydration process of blended cement

Tongsheng Zhang · Qijun Yu · Jiangxiong Wei · Peng Gao · Pingping Zhang

Received: 18 January 2011 / Accepted: 23 March 2011 / Published online: 8 April 2011

Abstract To optimize the hydration process of blended cement, cement clinker and supplementary cementitious materials (SCMs) were ground and classified into several fractions. Early hydration process of each cementitious materials fraction was investigated by isothermal calorimeter. The results show fine cement clinker fractions show very high hydration rate, which leads to high water requirement, while fine SCMs fractions present relatively high hydration (or pozzolanic reaction) rate. Cement clinker fractions in the range of 8–24 μm show proper hydration rate in early ages and continue to hydrate rapidly afterward. Coarse cement clinker fractions largely play "filling effect" and make little contribution to the properties of blended cement regardless of their hydration activity (or pozzolanic activity). The hydration process of blended cement can be optimized by arranging high activity SCMs, cement clinker, and low activity SCMs in fine, middle, and coarse fractions, respectively, which not only results in reduced water requirement, high packing density, and homogeneous, dense microstructure, but also in high early and late mechanical properties.

Keywords Blended cement · Hydration process · Heat evolution · Water requirement · Supplementary cementitious materials

T. Zhang · Q. Yu · J. Wei (✉) · P. Gao · P. Zhang
Key Laboratory of Specially Functional Materials of the Ministry of Education, South China University of Technology, Guangzhou 510640, China
e-mail: jxwei@scut.edu.cn

Introduction

There is an increasing worldwide trend toward utilization of pozzolanic (or cementitious) by-products either as a supplementary cementitious material (SCM) in manufacture of blended cement or as a mineral admixture in concrete mixing for engineering, ecological, and economic benefits [1]. And it is also a countermeasure to reduce CO_2 emission, substantial energy, and cost saving, because certain amount of energy costly cement clinker is replaced by SCMs. However, one shortcoming has not been solved perfectly, that is relatively low early strength of blended cements [2].

It is generally accepted that the properties of hardened cement paste are closely related to its porosity and pore size distribution [3], which mainly depend on packing density of fresh paste and filling effect of hydration products. Water requirement for normal consistency, which consists of filling water, chemically combined water, absorption water, and free water, has a crucial effect on packing density of fresh paste [4]. Filling water and absorption water are related to particle size distribution and specific surface area of cement, respectively. Chemically combined water is due to the surface hydration of cement particles in the first few minutes, while free water mainly contributes to fluidity of cement paste.

Since cement paste were mixed, the structure of cement paste is formed and becomes denser as hydration proceeds. If the hydration process of cement is too fast, high water requirement is always observed due to high chemically combined water, large amounts of hydration products with capillary pores are generated on the surface of cement particles at early ages. Limited hydration products generated in late ages can be found as Ca^{2+} can hardly diffuse through thick hydration products layer [5], thus the

microstructure is not as dense as desired. In contrast, if the hydration rate is relatively slow, a loosen microstructure is formed due to limited early hydration products though with low water requirement, the resulting consequence is poor early properties of cement paste. It can be deduced that a proper hydration process may lead to dense microstructure of hardened cement paste both in early and late ages.

Size fraction plays different roles in properties development during early and late ages. Fine clinker fraction (<3 μm) presents very high hydration activity, an increase of fine clinker fraction may results in higher early strength, but also cause high water requirement and undesirable volume changes [6, 7]. It has been reported that the clinker fraction in the range of 3–32 μm is the fraction which contributes most to strength development [8], while clinker particles coarser than 60 μm have only a "filling effect" and make practically no contribution to strength development [9]. Thus, the contents of fine and coarse fractions are both controlled in Portland cement production.

Different from Portland cement, blended cement contains both cement clinker (high activity) and SCM (low activity) or inert fillers. Hydration process of blended cement can be optimized by arranging the size range of clinker and SCMs (or inert fillers) according to their hydration process.

In present study, cement clinker and SCMs were ground and classified into several fractions, water requirement for normal consistency and hydration process of each cementitious materials fraction were characterized. Based on which the hydration process of blended cement was optimized, meanwhile the fundamental properties of the optimized blended cements were also performed as a validation. The study aims to optimize the hydration process of blended cement by arranging clinker and SCMs in proper size fractions. The results will be very useful to produce high performance blended cement with low clinker content and utilize SCMs and cement clinker more efficiently both in cement manufacture and concrete making.

Materials

Granulated blast furnace slag (GBFS), low calcium fly ash (a class F fly ash according to ASTM C 618 [10]), and steel slag (a by-product of steel converter) were used as SCMs, their chemical compositions are listed in Table 1. A Portland cement (CEM I 42.5) and ground SCMs were classified into several fractions by air classifier; particle size distribution parameters of all fractions measured by laser diffraction method (Malvern, Mastersizer 2000) are given in Table 2. Since particle size distribution of each SCMs fraction is similar to that of corresponding cement clinker fraction, only particle size distributions of seven cement clinker (CEM I 42.5) fractions are given in Fig. 1. As all fractions prepared have a narrow particle size distribution, D_{50} is taken as the mean size of each size fraction.

Water requirements for normal consistency of cementitious materials fractions

Water requirement for normal consistency of each cementitious materials' fraction were tested as specified in EN 196-3 [11], the results are shown in Fig. 2. For a given cementitious material, water requirement for normal consistency increases gradually as particle size gets finer. It should be noted for cementitious materials fractions finer than 10 μm, the water requirement increases significantly in parallel with the decreases of particle size, especially for cement clinker. For example, in comparison to clinker fraction with $D_{50} = 56.61$ μm, the water requirement of clinker fraction with $D_{50} = 16.19$ μm only increases by 39.7%, whereas that of clinker fraction with $D_{50} = 1.50$ μm increases by 208.0%. High water requirement of fine cementitious materials fractions can be attributed to the increase of chemically combined water and absorption water, which depend on inherent activity and surface properties of the cementitious materials, respectively.

Compared with fine clinker fractions, fine SCM fractions (<10 μm) need less water to achieve normal consistency, indicating the amount of chemically combined water caused by hydration or pozzolanic reaction of fine SCMs is much lower than that caused by hydration of fine clinker in the first few minutes. For middle fractions (10–30 μm), GBFS shows slightly higher water requirement than Portland cement, while steel slag presents much lower water requirement. No significant difference in water requirement is observed for coarse (>30 μm) clinker, GBFS, and steel slag fractions. In addition, low calcium fly ash presents relatively high water requirement due to high un-burnt carbon content (Table 1). It can be inferred that replacement of fine and coarse clinker fractions by corresponding SCM fractions may lead to reduced water requirement for normal consistency and high packing density of blended cement paste.

Hydration processes of cementitious materials fractions

It is proved that pore solution of Portland cement paste is similar to supersaturated $Ca(OH)_2$–0.2 mol/L NaOH solution [12]. Each cementitious materials fraction and CaO

Table 1 Chemical compositions of Portland cement, GBFS, low-calcium fly ash, and steel slag used in the experiment

Material	Chemical composition/%									
	SiO_2	Al_2O_3	Fe_2O_3	CaO	MgO	K_2O	Na_2O	SO_3	TiO_2	LOI
Portland cement	21.86	4.45	2.35	63.51	1.67	0.55	0.26	2.91	0.11	1.89
GBFS	35.22	12.15	0.25	37.08	11.25	0.49	0.25	1.19	0.73	−0.53
Low calcium fly ash	45.43	24.36	9.70	5.23	1.46	0.23	0.36	1.03	0.12	11.88
Steel slag	12.84	3.59	24.14	41.14	7.33	0.05	0.05	0.61	0.81	7.91

LOI loss on ignition

Table 2 Particle size distribution parameters of classified cementitious materials fractions

Fraction	C_1	C_2	C_3	C_4	C_5	C_6	C_7	G_1	G_2	G_3	G_4	G_5	G_6	F_1	F_2	F_3	F_4	F_5	S_1	S_2	S_3	S_4	S_5
D_{10}/μm	45.11	26.05	16.81	12.29	6.02	2.50	0.81	49.74	28.53	12.57	5.12	2.8	0.58	51.26	26.01	11.48	4.85	0.29	50.86	27.27	11.59	4.07	0.81
D_{50}/μm	56.61	33.37	21.48	16.19	7.81	3.98	1.50	54.84	32.27	16.08	6.31	4.72	1.67	58.85	31.38	17.39	6.43	1.45	55.27	31.73	15.17	5.74	1.43
D_{90}/μm	70.83	40.08	26.84	19.53	10.67	5.92	2.88	71.09	39.57	21.74	9.17	7.55	3.16	71.56	39.45	19.98	10.24	2.74	62.92	37.41	19.82	7.72	2.17

Note: C, G, F, and S represent cement clinker, GBFS, low calcium fly ash, and steel slag, respectively; D_{10}, D_{50}, and D_{90} are the maximum particle diameters when cumulative volume reaches 10, 50, and 90%, respectively

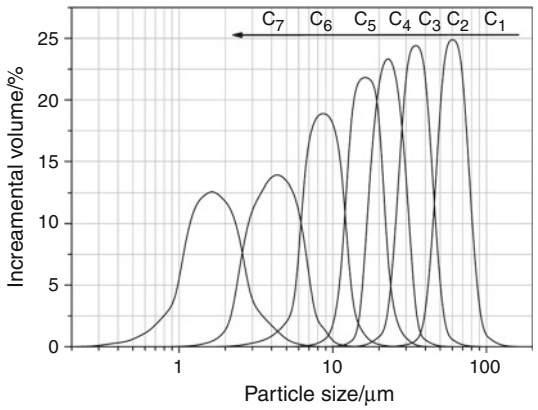

Fig. 1 Particle size distributions of classified Portland cement fractions

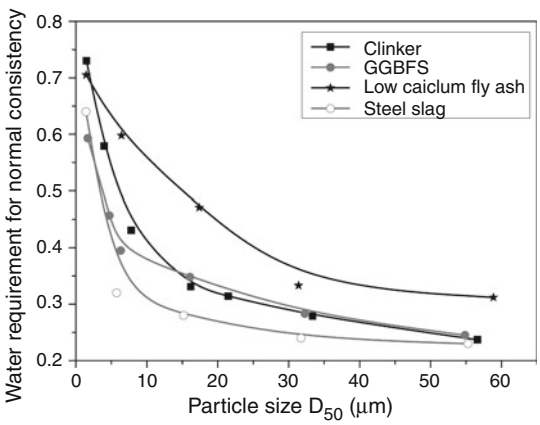

Fig. 2 Water requirements for normal consistency of classified cementitious materials fractions

were mixed with 0.2 mol/L NaOH solution into a paste of normal consistency according to proportions in Table 3, then heat evaluation of the obtained pastes was measured with an isothermal calorimeter (TAM air) according to ASTM C 1702-09 [13], the measurements were performed at constant temperature of 25 °C for 72 h. Meanwhile the pastes were sealed and cured at 20 ± 1 °C, the hydration products were observed by scanning electric microscope (SEM, Nano 430, 10 kV) at desired ages.

Hydration processes of cement clinker fractions

Figure 3 shows that clinker fraction with $D_{50} = 3.98$ μm presents high rate of heat evolution and cumulative heat of hydration, especially in the first 24 h, indicating that fine clinker particles have very high hydration rate. In contrast, clinker fractions in the range of 8–24 μm (such as $D_{50} = 16.19$ μm) show a proper hydration rate in the first 24 h and continues to hydrate rapidly afterward, the 3 days cumulative heat of hydration of which attains about 90% of that of the clinker fraction with $D_{50} = 3.98$ μm. Very low hydration rate and cumulative heat of hydration are observed for coarse Portland cement fractions (such as $D_{50} = 33.37$ μm). Large amounts of hydration products produce a loosen microstructure in the paste prepared by fine clinker fraction, and few hydration products generated from 24 h to 3 days can be found as shown in Fig. 4a and d. The paste prepared by middle clinker fraction presents a dense misconstrue due to low water requirement, and the microstructure becomes denser after 3 days curing (Fig. 4b, e).

Table 3 Mix proportions of cementitious materials pastes of normal consistency

Cementitious material		CaO/ wt%	Solution
Category	Proportion/ wt%		
Cement clinker fraction	100	0	Water
Fly ash fraction	90	10	0.2 mol/L NaOH
GBFS fraction	90	10	0.2 mol/L NaOH
Steel slag fraction	100	0	0.2 mol/L NaOH

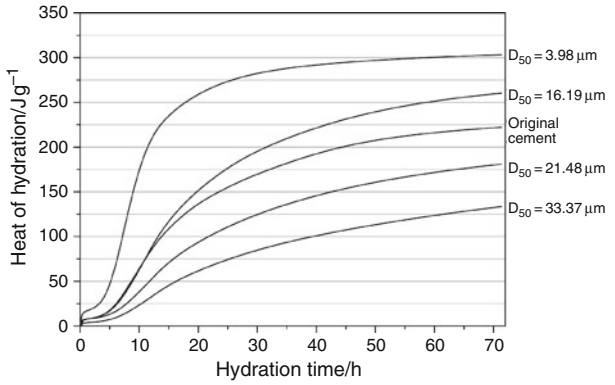

Fig. 3 Heat evolution of pastes prepared by classified Portland cement fractions

Figure 4c and f shows very limited hydration products, and large amount of un-hydrated clinker particles are found in the paste prepared by coarse clinker fraction.

Hydration processes of GBFS fractions

Figure 5 depicts that heat evolution of GBFS pastes is similar to that of clinker pastes. The rate of heat evolution of GBFS pastes has two exothermal peaks, but the first peak mainly attributes to rapid reaction of CaO with water immediately after mixing of GBFS pastes and the second peak corresponds to pozzolanic reaction of fine GBFS particles [14]. Fine GBFS fraction with $D_{50} = 1.67$ μm presents much higher value for the two exothermal peaks compared with coarse GBFS fractions (such as $D_{50} = 16.08$ μm), indicating pozzolanic reaction of fine GBFS particles initiates forward and is with high rate. GBFS fractions with $D_{50} = 4.70$ μm and 6.31 μm also present relatively higher cumulative heat of hydration. For GGBFS pastes prepared by fine or middle fractions, certain amounts of hydration products are observed after 3 days curing (Fig. 6a, b), and the amounts of hydration products increase significantly after 28 days curing (Fig. 6d, e). While coarse GBFS fractions have only surface hydrated after 28 days curing (Fig. 6c, f).

Hydration processes of fly ash fractions

Figure 7 shows that fly ash fraction with $D_{50} = 1.45$ μm presents a much higher rate of heat evolution and cumulative heat compared with other fractions. Figure 8a shows surface disintegration of small fly ash particles and amounts of hydration products generated on the surface of fly ash particles are observed after being cured for 3 days, indicating the initiation of pozzolanic reaction [15]. The amounts of hydration products increase remarkably after 28 days curing as shown in Fig. 8d. In contrast, pozzolanic reaction of middle and coarse fly ash fractions can be

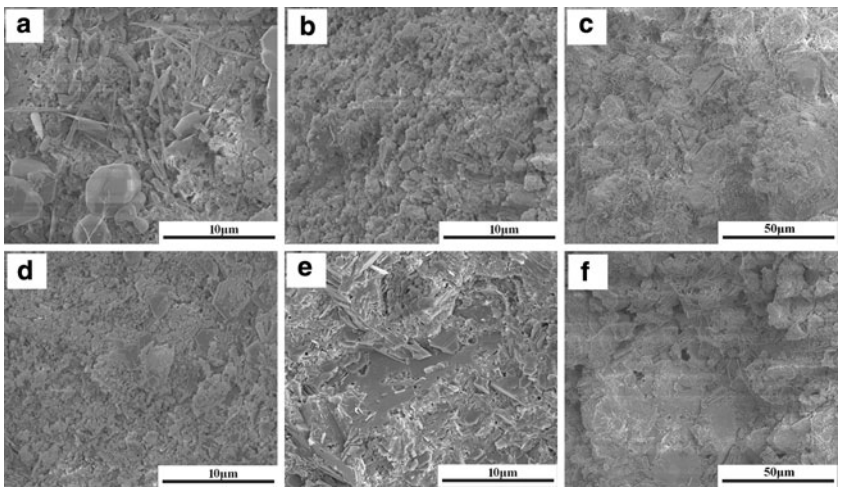

Fig. 4 SEM images of hardened pastes prepared by classified cement clinker fractions. **a** Fine fraction ($D_{50} = 3.98$ μm) cured for 24 h; **b** middle fraction ($D_{50} = 16.19$ μm) cured for 24 h; **c** coarse fraction ($D_{50} = 33.37$ μm) cured for 24 h; **d** fine fraction ($D_{50} = 3.98$ μm) cured for 3 days; **e** middle fraction ($D_{50} = 16.19$ μm) cured for 3 days; **f** coarse fraction ($D_{50} = 33.37$ μm) cured for 3 days

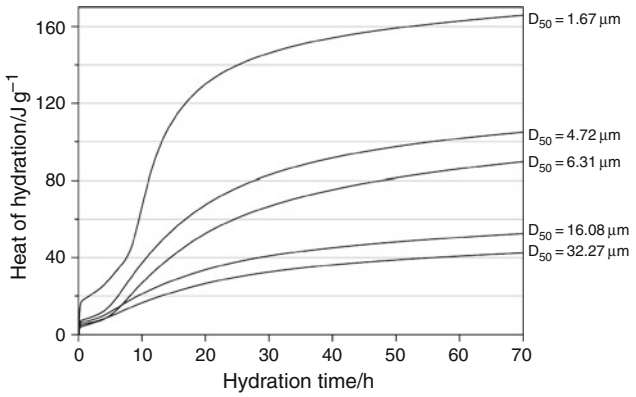

Fig. 5 Heat evolution of pastes prepared by classified GBFS fractions

neglected in the first 3 days (Fig. 8b, c), and few hydration products are observed after 28 days curing (Fig. 8e, f).

Hydration processes of steel slag fractions

Figure 9 shows no obviously difference in heat evolution was observed for steel slag fractions coarser than 5 μm. In contrast, steel slag fraction with D_{50} = 1.43 μm presents a much higher rate of heat evolution and cumulative heat of hydration. Figure 10a depicts large amount of hydration products are observed in the paste prepared by fine steel slag fraction (D_{50} = 1.43 μm) after 3 days curing. While steel slag fraction with D_{50} = 5.74 μm shows slightly hydration (Fig. 10b), and coarse steel slag particles remain "clean" surface after 3 days curing (Fig. 10c). The pate prepared by fine steel slag fraction shows large amounts of hydration products after 28 days curing (Fig. 10d), while the amounts of hydration products are very limited in pastes prepared by middle or coarse steel slag fractions (Fig. 10e, f).

Optimization of hydration process of blended cement through arranging cementitious materials according to their hydraulic (or pozzolanic) activity

The hydraulic (or pozzolanic) activity of a given cementitious material particle depends on its inherent activity and particle size (or specific surface area). Cement clinker presents higher inherent activity than SCM, and GBFS generally shows relatively higher inherent activity compared with fly ash. As cementitious materials particles get finer, the hydration (or pozzolanic reaction) increases significantly due to larger chemical reaction area. Furthermore, activity difference can sometimes be attributed to deviation of mineral compositions occured during grinding and classifying process. Such as, an increased amount of C_3S is found in fine Portland cement fraction [16], and a larger amount of silicates and a greater proportion of ferrites are observed in fine and coarse steel slag fractions, respectively [17]. Therefore, fine cementitious materials fractions always show dramatically higher hydraulic (or pozzolanic) activity than corresponding coarse fractions.

The activity of each cementitious materials fraction should be controlled in a certain range to avoid high water requirement and low properties contribution. Fine cement clinker fractions present high water requirement and limited properties contribution due to rapid hydration rate. Middle cement clinker fractions have low water requirement and appropriate hydration rate at early ages, thus these fractions play dominant contribution to the properties development of blended cement. Coarse fractions largely

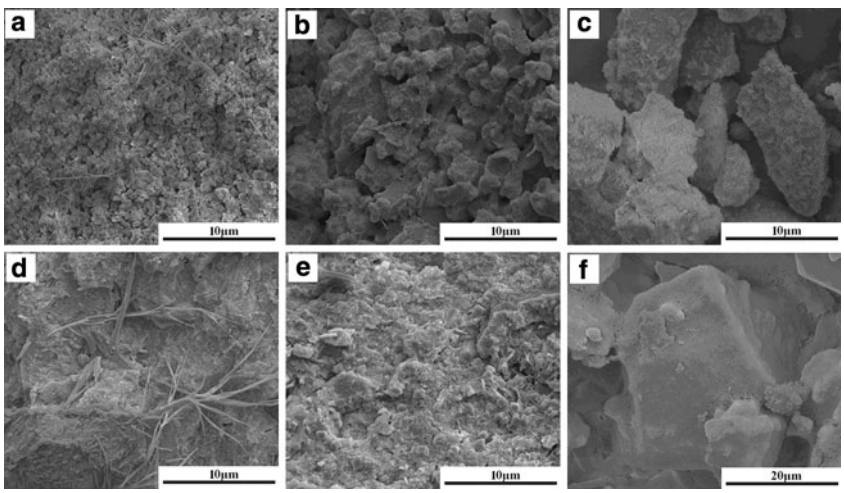

Fig. 6 SEM images of hardened pastes prepared by classified GBFS fractions. **a** Fine fraction (D_{50} = 1.67 μm) cured for 3 days; **b** middle fraction (D_{50} = 6.31 μm) cured for 3 days; **c** coarse fraction (D_{50} = 16.08 μm) cured for 3 days; **d** fine fraction (D_{50} = 1.67 μm) cured for 28 days; **e** middle fraction (D_{50} = 6.31 μm) cured for 28 days; **f** coarse fraction (D_{50} = 16.08 μm) cured for 28 days

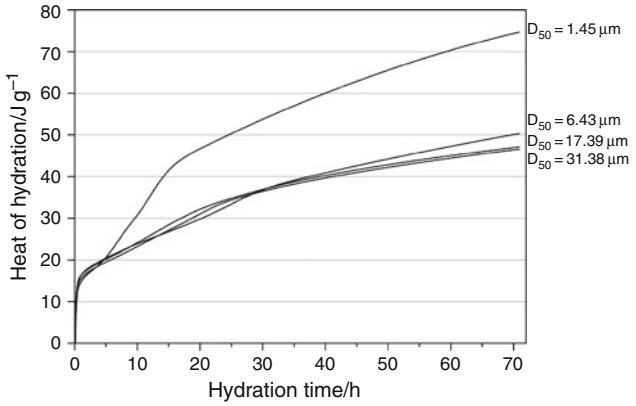

Fig. 7 Heat evolution of pastes prepared by classified low calcium fly ash fractions

play "filling effect" and make little contribution to the properties of blended cement regardless of their hydration activity (or pozzolanic activity). Thus, the relatively costly cement clinker is being wasted in both fine and coarse fractions and can be replaced by SCMs, which results not only in reduced water requirement, but also in maximum properties contribution. More sustainable blended cement can be achieved as largely partial of cement clinker is replaced by industrial by-products with no or little properties loss.

Fundamental properties of optimized blended cements

To optimize the hydration process of blended cement and utilize cementitious materials more efficiently, both fine and coarse clinker fractions are replaced by high activity SCMs and low activity SCMs, respectively. The optimized blended cements and a Portland cement (CCCCC) were prepared by mixing clinker fractions and SCM fractions homogeneously according to mix proportions in Table 4. A reference cement consisting of 36% GBFS, 25% clinker, and 39% fly ash was also prepared by co-grinding, the Blaine specific surface area of the reference cement is controlled in the range of 350–360 m^2/kg, which is in agreement to that of optimized blended cements.

Packing densities of optimized blended cement pastes

Water requirements for normal consistency of optimized blended cements were determined according to EN 196-1 [18]. Maximum volume concentration of solids is used to characterize the packing density of cement pastes [19]. The obtained cements were mixed with water at different W/C ratios, and then density of the wet paste was measured. For the maximum density of wet paste ρ_{wet}, the maximum

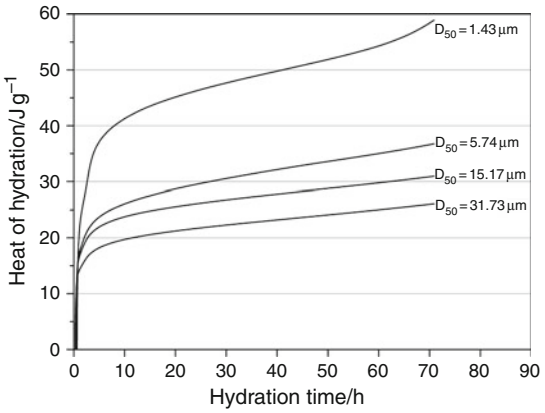

Fig. 9 Heat evolution of pastes prepared by classified steel slag fractions

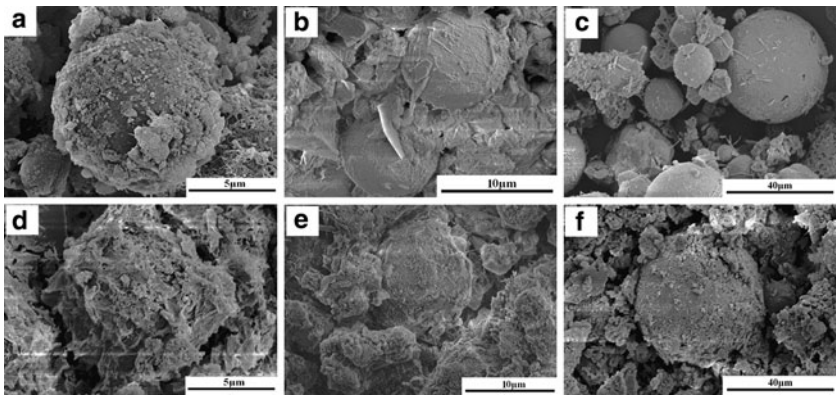

Fig. 8 SEM images of hardened pastes prepared by classified low calcium fly ash fractions. **a** Fine fraction (D_{50} = 1.45 μm) cured for 3 days; **b** middle fraction (D_{50} = 6.43 μm) cured for 3 days; **c** coarse fraction (D_{50} = 17.39 μm) cured for 3 days; **d** fine fraction (D_{50} = 1.45 μm) cured for 28 days; **e** middle fraction (D_{50} = 6.43 μm) cured for 28 days; **f** coarse fraction (D_{50} = 17.39 μm) cured for 28 days

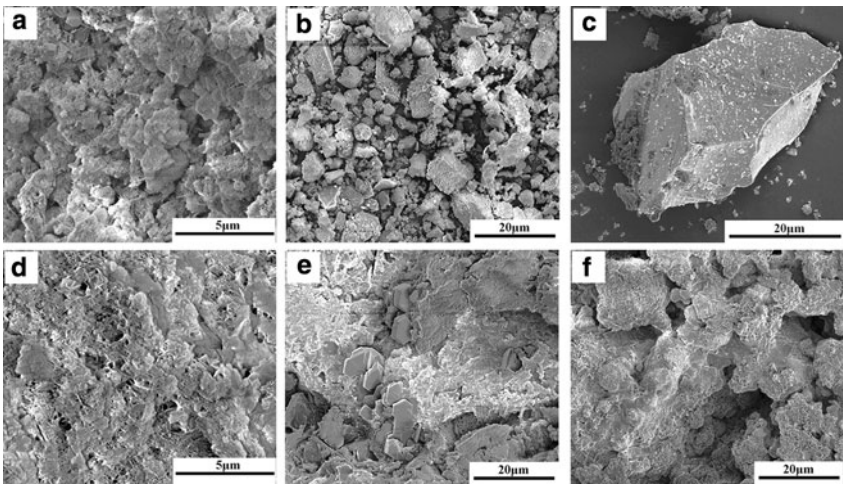

Fig. 10 SEM images of hardened pastes prepared by classified steel slag fractions. **a** Fine fraction (D_{50} = 1.43 μm) cured for 3 days; **b** middle fraction (D_{50} = 5.74 μm) cured for 3 days; **c** coarse fraction (D_{50} = 15.17 μm) cured for 3 days; **d** fine fraction (D_{50} = 1.43 μm) cured for 28 days; **e** middle fraction (D_{50} = 5.74 μm) cured for 28 days; **f** coarse fraction (D_{50} = 15.17 μm) cured for 28 days

Table 4 Mix proportions of optimized blended cements

Fractions/μm	<4	4–8	8–24	24–45	45–80
Content/vol.%	25	11	25	19	20
GGCFF	G (GBFS)	G (GBFS)	C (Cement clinker)	F (Fly ash)	F (Fly ash)
GGCSS	G (GBFS)	G (GBFS)		S (Steel slag)	S (Steel slag)
GGCGG	G (GBFS)	G (GBFS)		G (GBFS)	G (GBFS)
CCCCC	C (Cement clinker)	C (Cement clinker)		C (Cement clinker)	C (Cement clinker)
Reference cement	36% GGBFS + 25% Cement clinker + 39% Fly ash				

Note: The SO_3 content of all cements in Table 4 is controlled ~3%

Table 5 Maximum volume concentrations of solids of optimized blended cement pastes

Cement	GGCFF	GGCSS	GGCGG	CCCCC	Reference cement
Water requirement for normal consistency	0.334	0.316	0.317	0.331	0.356
Specific density/g/cm^3	2.816	3.211	2.824	3.150	2.870
Maximum wet density/g/cm^3	2.010	2.247	2.028	2.056	1.849
Maximum volume concentration of solids/%	55.62	56.42	56.37	49.12	45.40

volume concentration of solids φ of the cement pastes can be calculated by Eq. 1:

$$\varphi = \frac{\rho_{wet} - \rho_w}{\rho_c - \rho_w}, \quad (1)$$

where ρ_w and ρ_c are the densities of water and cement, respectively.

Due to grain size refinement and optimized hydration process, Table 5 shows that optimized blended cements present much lower water requirement for normal consistency and higher maximum volume concentration of solids than reference cement and CCCCC cement. For example, the maximum volume concentration of solids of GGCFF cement paste can be as high as 55.62%, which is increased by 10.22% than that of reference cement (45.40%). The results prove that the optimized blended cement pastes show high packing density.

Mechanical properties of optimized blended cements

Figure 11a shows that both 3 and 28 days compressive strengths of optimized blended cements are much higher than that of reference cement and can be comparable with that of CCCCC cement. For instance, although with same

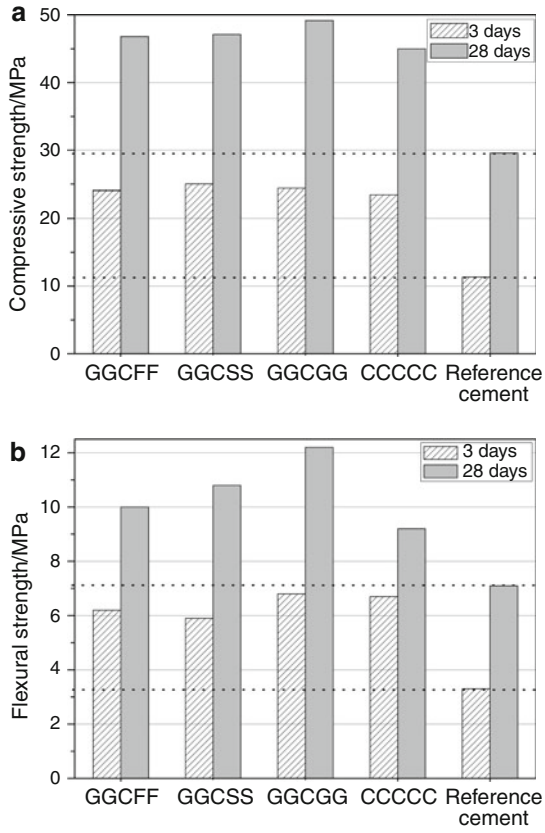

Fig. 11 Compressive and flexural strengths of optimized blended cements. **a** Compressive strength and **b** flexural strength

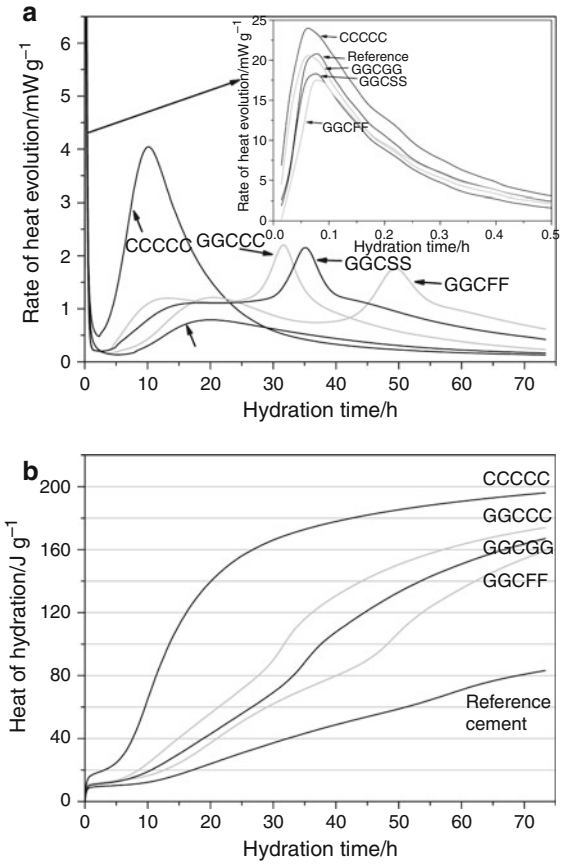

Fig. 12 Heat evolution of optimized blended cement pastes. **a** Rate of heat evolution and **b** cumulative heat of hydration

mix proportion, GGCFF cement has a 3- and 28-day compressive strength of 24.1 and 46.8 MPa, which is increased by 113.3 and 58.1%, respectively, compared with that of reference cement. Figure 11b demonstrates that optimized blended cements also present high flexural strength.

Heat evolution and microstructure of optimized blended cement pastes

Heat evaluation of the optimized blended cement pastes of normal consistency was measured with an isothermal calorimeter, and the microstructure of hardened pastes was observed by SEM at desired ages.

Different from heat evolution of CCCCC cement paste and reference cement paste, an additional peak in the range of 25–60 h, which attributes to pozzolanic reaction of fine GBFS particles, is observed as shown in Fig. 12, suggesting pozzolanic reaction of fine GBFS particles in optimized blended cements takes place after 24 h and is much more significance than that in reference cement. In addition, the first peak (around 0.1 h) and second peak (in the range of 10–20 h) of heat evolution, which correspond to hydration of clinker particles [20], are much lower than that of CCCCC cement due to replacement of fine and coarse clinker fractions by corresponding SCM fractions. As a result, most of heat of hydration of CCCCC cement is released in the first 24 h, while that of optimized blended cements releases slowly in the first 24 h and continues to increase rapidly afterward.

Very limited hydration products and large amount of un-hydrated particles are observed in reference cement paste (Fig. 13a, b). In addition, obvious gaps among un-hydrated particles and hydration products are found after being cured for 28 days (Fig. 13c). Large amounts of hydration products with capillary pores are observed in CCCCC cement paste cured for 24 h (Fig. 13d), and these capillary pores are still existed though few large-sized pores are left in CCCCC cement paste cured for 28 days (Fig. 13e, f). Certain amounts of hydration products produce a dense microstructure in optimized blended cement paste as shown in Fig. 13g. Hydration products increase steadily and bound with un-hydrated particles firmly as hydration proceeds (Fig. 13h). The microstructures of optimized

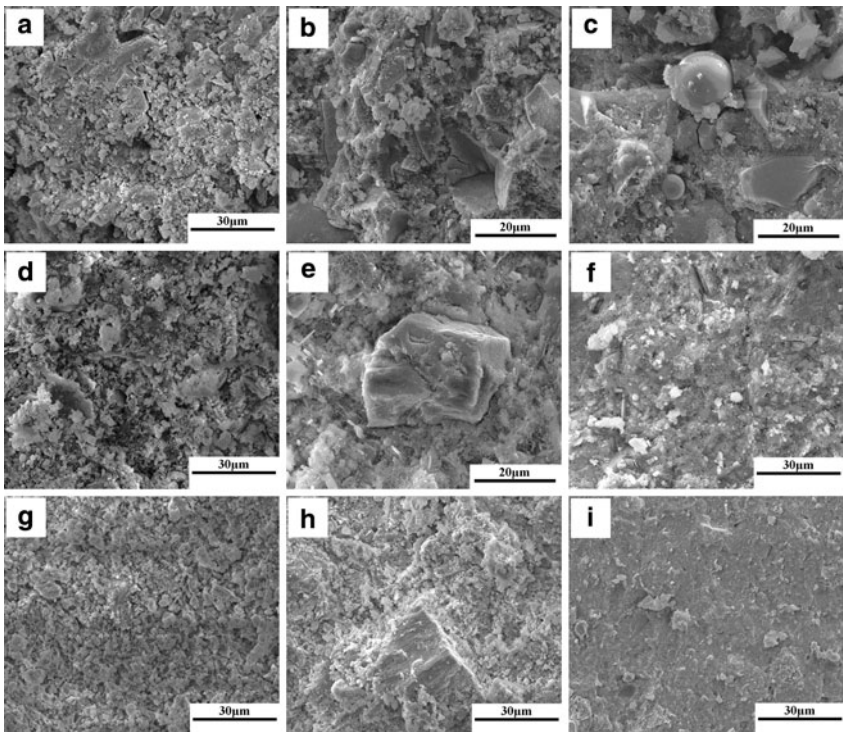

Fig. 13 SEM images of hardened optimized blended cement pastes. **a** Reference cement paste cured for 24 h, **b** reference cement paste cured for 3 days, **c** reference cement paste cured for 28 days, **d** Portland cement paste cured for 24 h, **e** Portland cement paste cured for 3 days, **f** Portland cement paste cured for 28 days, **g** GGCSS cement paste cured for 24 h, **h** GGCSS cement paste cured for 3 days, and **i** GGCSS cement paste cured for 28 days

blended cement pastes become denser and few capillary pores are found after 28 days curing (Fig. 13i).

Conclusions

The main conclusions that can be drawn from this experimental study are summarized as follows:

(a) Replacement of fine and coarse Portland cement fractions by corresponding SCM fractions may lead to reduced water requirement for normal consistency and high packing density of blended cement paste.

(b) Fine cement clinker fractions show very high hydration rate, which leads to high water requirement, while fine SCM fractions present relatively high hydration (or pozzolanic reaction) rate. Portland cement fractions in the range of 8–24 μm show proper hydration rate in early ages and continue to hydrate rapidly afterward. Coarse fractions largely play "filling effect" and make little contribution to the properties of blended cement regardless of their hydration activity (or pozzolanic activity).

(c) The hydration process of blended cement can be optimized by arranging high activity SCMs, cement clinker, and low activity SCMs in fine, middle, and coarse fractions, respectively, which not only results in reduced water requirement, high packing density and homogeneous, dense microstructure, but also in high early and late mechanical properties.

Acknowledgements This work was funded by 973 National Foundational Research of China (No. 2009CB623104), National Natural Science Foundation of China (No. 51072058), and Fundamental Research Funds for the Central Universities (No. 2009ZZ004), and their financial support is gratefully acknowledged.

References

1. Malhotra VM, Metha PK. Pozzolanic and cementitious materials. London: Gordon and Breach Press; 1996.
2. Altun IA, Yilmaz I. Study on steel furnace slags with high MgO as additive in Portland cement. Cem Concr Res. 2002;32:1247–9.
3. Wang AQ, Zhang CZ, Zhang NS. The theoretic analysis of the influence of the particle size distribution of cement system on the property of cement. Cem Concr Res. 1999;29:1721–6.
4. Wang AQ, Zhang CZ, Sun W. Fly ash effects: the morphological effect of fly ash. Cem Concr Res. 2003;33:2023–9.
5. Snellings R, Mertens G, Elsen J. Calorimetric evolution of the early pozzolanic reaction of natural zeolites. J Therm Anal Calorim. 2010;101:97–105.
6. Gruyaert E, Robeyst N, De Belie N. Study of the hydration of Portland cement blended with blast-furnace slag by calorimetry and thermogravimetry. J Therm Anal Calorim. 2010;102:941–51.
7. Škvára F, Kolár K, Novotný J. The effect of cement particle size distribution upon properties of pastes and mortars with low water-to-cement ratio. Cem Concr Res. 1981;11:247–55.
8. Tsivilis S, Tsinmas S, Benetatou A. Study on the contribution of the fineness on cement strength. Zem Kalk Gips. 1990;1:26–9.
9. Celik IB. The effects of particle size distribution and surface area upon cement strength development. Powder Technol. 2009;188:272–6.
10. ASTM C 618-03. Standard specification for coal fly ash and raw or calcined natural pozzolan for use as a mineral admixture in Portland cement concrete. American Society for Testing and Materials; 2003.

11. EN196-3. Methods of determination of water requirement for normal consistency. European Standards; 1997.
12. Lothenbach B, Winnefeld F, Alder C, Wieland E. Effect of temperature on the pore solution, microstructure and hydration products of Portland cement pastes. Cem Concr Res. 2007;37:483–91.
13. ASTM C 1702-09A. Standard test method for measurement of heat of hydration of hydraulic cementitious materials using isothermal conduction calorimetry. American Society for Testing and Materials; 2009.
14. L'ubomír J, Marin P, Jana K, TomáŠ I. Determination of activation effect of $Ca(OH)_2$ upon the hydration of BFS and related heat by isothermal calorimeter. J Therm Anal Calorim. 2010;101:585–93.
15. Pacewska B, Blonkowski G, Wilińska I. Investigation of the influence of different fly ashes on cement hydration. J Therm Anal Calorim. 2006;86:179–86.
16. Zhang TS, Yu QJ, Wei JX, Zhang PP. Effects of size fraction on composition and fundamental properties of Portland cement. Constr Build Mater. 2011. doi:10.1016/j.conbuildmat.2011.01.005.
17. Shi CJ. Steel slag—its production, processing, characteristics, and cementitious properties. J Mater Civ Eng. 2004;16:230–6.
18. EN 196-1. Methods of determination of strength. European Standards; 1997.
19. Kwan AKH, Fung WWS. Packing density measurement and modeling of fine aggregate and mortar. Cem Concr Compos. 2009;31:349–57.
20. Mostafa NY, Brown PW. Heat of hydration of high reactive pozzolans in blended cements: isothermal conduction calorimetry. Thermochim Acta. 2005;435:162–7.